

Project on AC corrosion conducted at:
Department of Manufacturing Engineering, Materials Technology, Building 204,
The Technical University of Denmark, DK-2800 Lyngby, Denmark

Funded by:
DONG Natural Gas A/S. Agerø Allé 24-26, DK-2970 Hørsholm, Denmark.

August 2000

AC Corrosion Rates of Cathodically Polarised Steel Exposed in a Scaling, Neutral pH Soil Solution

Lars Vendelbo Nielsen
lvn@ipt.dtu.dk

Keywords:

Cathodic polarisation, cathodic scaling, spread resistance, AC current density, ER-technique, corrosion rate.

Abstract

In an artificial solution with a capability of forming cathodic scaling throughout time, the corrosion rate of steel has been studied by the ER-technique under conditions with controlled AC and DC voltage as well as with controlled AC and DC current.

The resulting AC current density in the controlled voltage experiments showed that the AC current density decreased throughout time due to development of increased spread resistance caused by the cathodic scaling. The scaling and accordingly the increase in spread resistance developed faster when increasing the degree of cathodic protection (DC potential -850 mV SCE versus -1000 mV SCE). The corrosion rate decreased throughout time as the AC current decreased due to the increased spread resistance. The controlled current experiments were initiated in order to study the corrosion rate when the AC current in particular was held constant (5 levels from 10 - 1000 A/m² was superimposed onto the constant DC of 1 A/m²). From these experiments, the thesis that the AC current density can be used to assess the degree of the AC corrosion risk was tested. The measured corrosion rates were found to fit into the general equation $\log(V_{Corr}) = -A + B \cdot \log(i_{AC})$.

In the controlled current experiments, the initial corrosion rate was around one decade higher than the corrosion rate after 15h (representing values closer to a steady state condition), but both initial- and final corrosion rate was found to increase with increasing AC current density following said equation. The corrosion rates measured in the controlled voltage experiments were found to be located in the range as defined by the controlled current experiments.

Introduction

Discussions on corrosion mechanisms in cathodically protected pipelines superimposed by an AC-voltage often involve effects of factors like spread resistance, level of the AC current density, and maximum anodic iR -free peak potentials.¹⁻³ These quantities are accordingly used as guideline parameters for assessments of the risks of AC corrosion in pipelines. Gregoor and Pourbaix³ put forward that when the instant iR free potential (anodic peak potential) oversteps -800 mV SCE, the possibility of corrosion is present. Accordingly, they conclude that if the anodic peak potential is permanently below this value, corrosion is not a problem. The present investigation briefly deals with this parameter, but focuses primarily on the effect of the AC current density on corrosion. It is normally suggested that when the AC current density is lower than 30 A/m², the pipeline is not susceptible to AC corrosion.

Experimental

Two series of experiments were conducted in identical electrochemical three-electrode arrangements established in 2-liter glass vessels each equipped with a 2-cm² steel sample as working electrode, a large (500 cm²) titanium-mesh as counter electrode, and a saturated calomel electrode (SCE, +0.242 V vs. SHE) as reference electrode.

Both series were conducted in a nitrogen-purged solution with chemical composition according to table 1. This solution is denoted “scaling solution”, since it has previously been used as a solution forming cathodic scaling when the steel electrode was cathodically polarised for an extended period of time.^{4,5}

Component	Concentration (mg/L)	Concentration (mol/L)
MgSO ₄ , 7H ₂ O	617	$2.5 \cdot 10^{-3}$
CaSO ₄ , 2H ₂ O	430	$2.5 \cdot 10^{-3}$
NaHCO ₃	210	$2.5 \cdot 10^{-3}$
CaCl ₂	554	$5.0 \cdot 10^{-3}$

Table 1. Chemical composition of the scaling solution applied in the experimental series. Initial pH = 7.8, initial conductivity = 1900 μ S/cm.

In the first experimental series, the steel electrode was polarised by controlled AC- and DC voltage, and for this purpose, the electrical set-up illustrated in figure 1 was employed. A 50-Hz AC transformer fed a potentiostat with an AC voltage hereby superimposed onto the DC-potential controlled by said potentiostat. A Ramlog recorder (the principles of which has been described elsewhere^{3,5}) was inserted in the circuit for measurements of average ON-potential, instant OFF-potential, and instant current values every other minute throughout the test periods. A fluke multimeter was used to control the current and voltage characteristics frequently throughout the tests.

The working electrode was designed as an ER-probe connected via an ER-instrument, measuring changes of the electrical resistance of the 25- μm thick steel foil being part of the ER-probe. The temperature-compensated changes of the electrical resistance were measured with a resolution of tenth of a $\mu\Omega$, allowing for very quick measurements of corrosion rate according to the equation:^{6,7}

$$V_{\text{corr}} = \frac{dR}{dt} \cdot \frac{\rho}{R^2} \cdot \frac{L}{W} \quad (1)$$

where L is length of the probe element, W is width of probe element, ρ is specific resistivity of the element material, and R is element resistance.

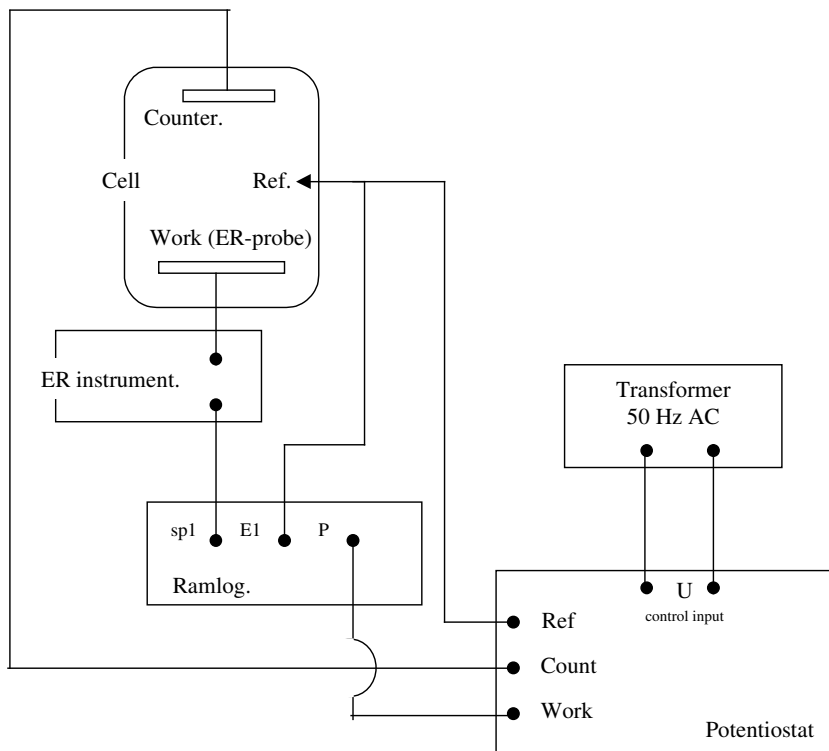


Figure 1. Electric diagram used for the potentiostatic AC- and DC-charging of the ER-probe.

In the first experiment in this series, the DC-potential (“ON”-condition) was kept at -850 mV SCE, superimposed by 2.12 V AC (RMS). This condition was kept for a 70h test period, throughout which the corrosion rate was measured. In the second experiment, the DC-potential (“ON”-condition) was kept at -1000 mV SCE, superimposed by 2.12 V AC (RMS). This condition was kept for a 15h test period, throughout which the corrosion rate was measured.

In the second experimental series, the steel electrode was polarised by controlled AC- and DC current, and for this purpose, the electrical set-up illustrated in figure 2 was employed. A 50-Hz AC transformer fed a potentiostat coupled as a galvanostat by the

resistor inserted in between the “Ref”- and “Work” terminals, hereby creating an AC-galvanostat. A similar DC galvanostat was established, and the AC- and DC current accordingly supplied to the electrode system via individual AC- and DC galvanostats separated from each other separated (ensuring no leak of DC through the AC galvanostat) by a large capacitance (20 mF) inserted in the counter circuit. Again, a Ramlog recorder was applied for measurements of average ON-potential, instant OFF-potential, and instant current values every other minute throughout the test period. The ER-technique was employed for measurements of the instant corrosion rate throughout time. The galvanostatic experiments involved a constant DC charging of 1 A/m^2 (cathodic), whereas 10, 30, 100, 300, and 1000 A/m^2 AC current was superimposed onto this DC current in 5 individual experiments. Each experiment was maintained for approximately 15 hours, except the 1000 A/m^2 experiment in which the ER-probe was totally corroded after short time exposure (2 hours).

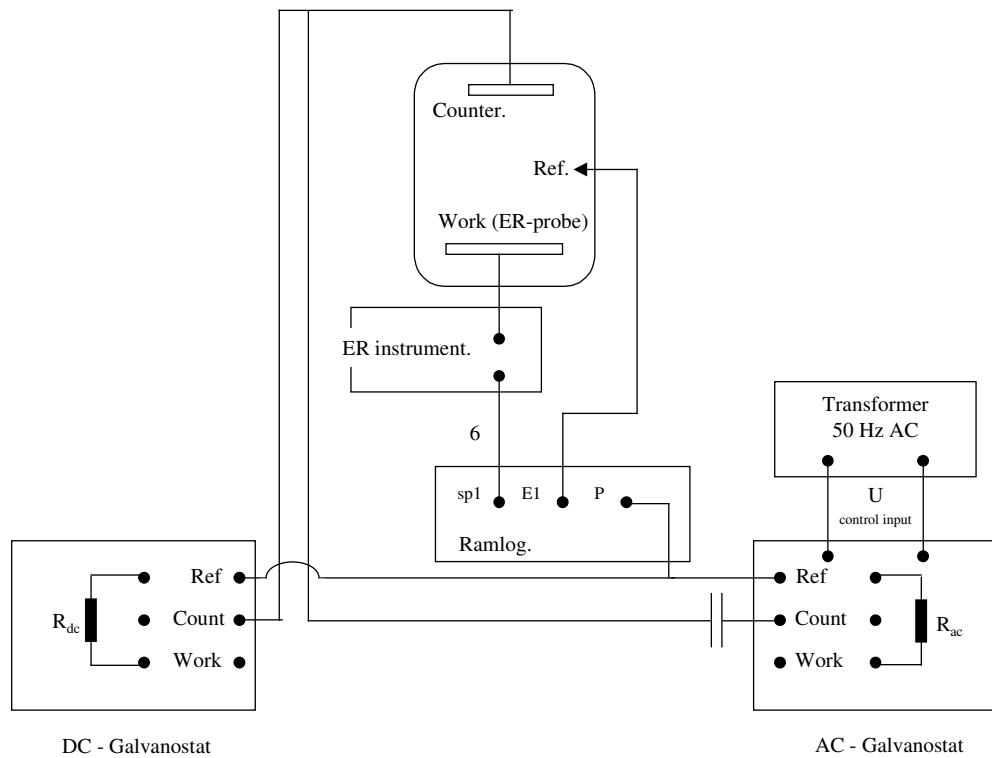


Figure 2. Electric diagram used for the galvanostatic AC- and DC-charging of the ER-probe.

Results and discussion

Potentiostatic experiments

Figure 3 illustrates the instant current values measured throughout time by the Ramlog recorder in the 70h experiment (DC = -850 mV SCE, AC = 2.12 V RMS), and in figure 4 the current recorded in the 15h test (DC = -1000 mV SCE, AC = 2.12 V RMS) is shown. As justified elsewhere,⁴ the RMS AC current can be extracted from these Ramlog recordings according to the equation:

$$i_{AC,RMS} = \frac{\max(i_n \dots i_{n+x}) - \min(i_n \dots i_{n+x})}{2 \cdot \sqrt{2}} \quad (2)$$

where $\max(i_n \dots i_{n+x})$ and $\min(i_n \dots i_{n+x})$ denotes the maximum and minimum current respectively measured throughout x ($= 30$ in the present investigation) current measurements. Dividing this value by 2 gives the current amplitude, and dividing by $\sqrt{2}$ gives the RMS value. The RMS AC currents so calculated are shown for the two experiments in figure 5.

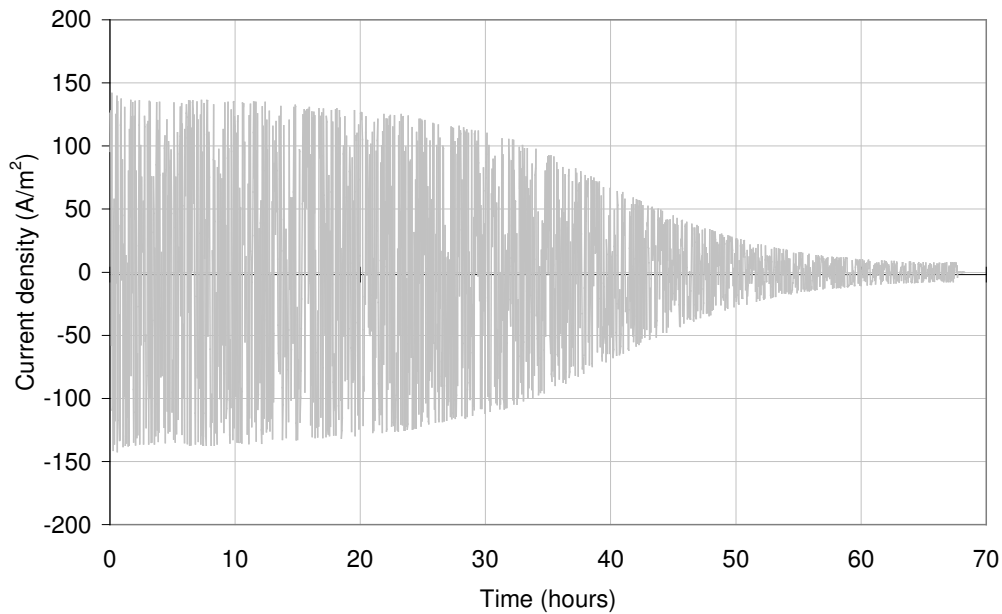


Figure 3. Ramlog recordings of the instant current throughout time, 70h experiment (DC = -850 mV SCE, AC = 2.12 V RMS).

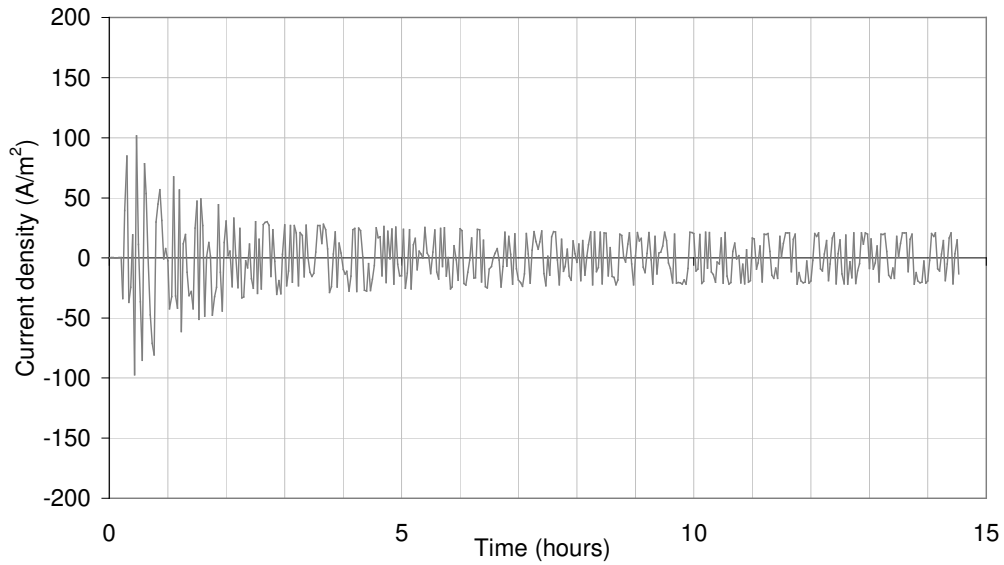


Figure 4. Ramlog recordings of the instant current throughout time, 15h experiment (DC = -1000 mV SCE, AC = 2.12 V RMS).

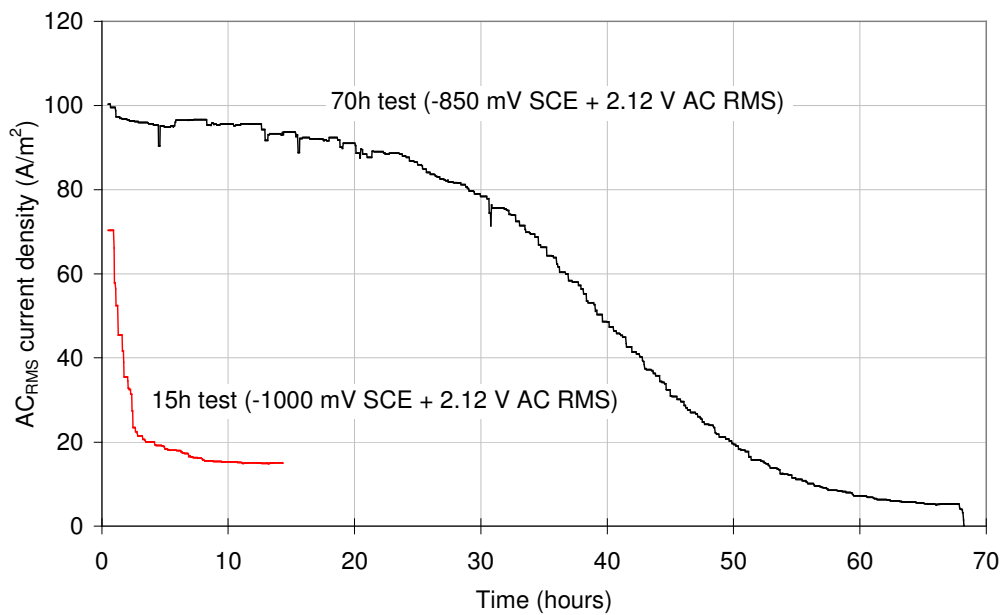


Figure 5. Comparison of the AC current densities developed in the potentiostatic experiments.

As observed from figure 5, the AC current density decreases throughout time in both experiments, but quite more rapidly when the DC offset potential is shifted in the cathodic direction. The reason for this behaviour is probably an increase in the spread resistance R_S caused by the development of cathodic scaling products as justified in earlier studies.⁵

The development in the spread resistance can be assessed from the Ramlog measurements according to the following equation:⁵

$$R_s = \frac{U_{AC,ON,RMS} - U_{AC,OFF,RMS}}{i_{AC,RMS}} \quad (3)$$

where $U_{AC,ON,RMS}$ is the controlled AC voltage (2.12 V RMS) and $U_{AC,OFF,RMS}$ is the iR-free RMS voltage calculated from the Ramlog recording analogous to the i_{RMS} calculation (equation (3)). It is recognised that the R_s calculation according to equation (3) introduces a minor error due to phases between current and voltage, but as justified previously this does not disturb the general impression significantly.⁵ The spread resistance so calculated is illustrated for the two experiments in figure 6, showing that the increase in spread resistance takes place in both experiments, but quite more rapidly in the 15h experiment with strongest cathodic protection. The CP produces alkalinity (OH⁻) which in turn reacts with the earth alkaline cations (Ca²⁺ and Mg²⁺).

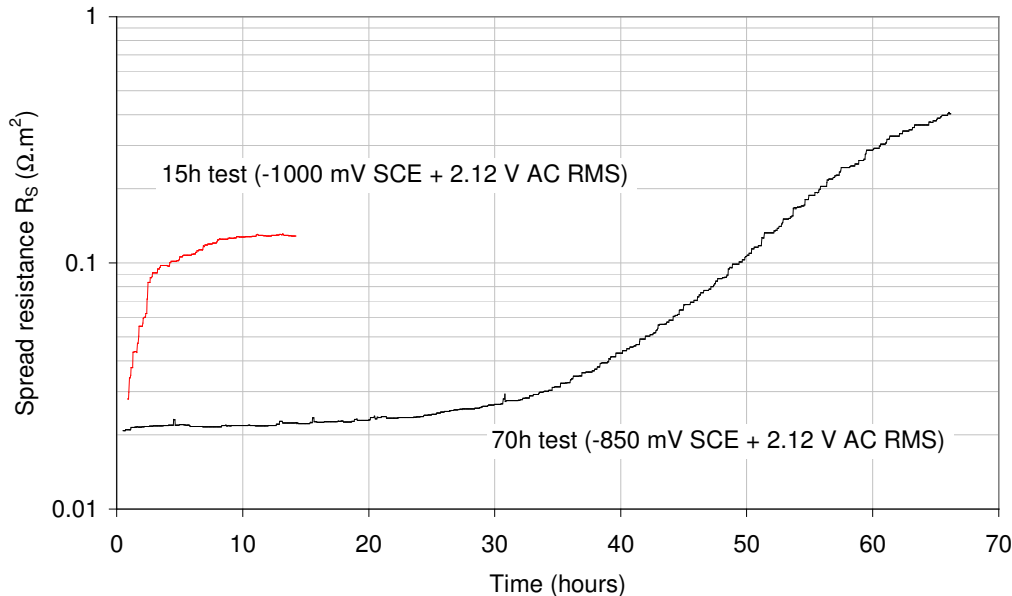


Figure 6. Calculated spread resistance throughout time in the potentiostatic experiments.

The changes of the resistance of the ER-probes with time ($R - R_0$, where R_0 is initial resistance) in general provided quite plausible curves, which is illustrated in figure 7 for the 70h test as an example. Using equation (1) directly as the resistance change with a 2-minute interval gives the corrosion rate, which is also illustrated in the figure.

The fact that the ER-technique can be applied as a real time measurement makes it possible to compare the corrosion rate throughout time with developments in other parameters. The perhaps most interesting of these is the AC current density, which - as previously mentioned - is used as a guideline parameter when assessing the risk of AC-corrosion. Since in these potentiostatic experiments, the AC current density decreases throughout time due to increasing spread resistance, the experiments can be used to make a preliminary judgement of the influence of the AC current density on

the corrosion rate. Figure 8 illustrates the Corrosion rate versus AC current density for the potentiostatic experiments.

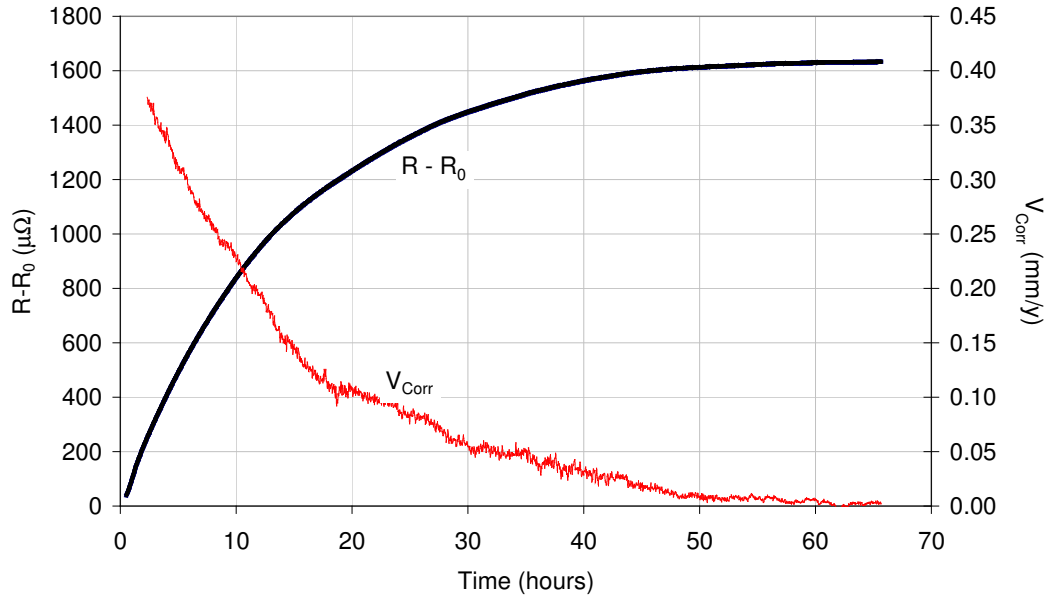


Figure 7. Changes of the ER-probe resistance with time throughout the 70h test.

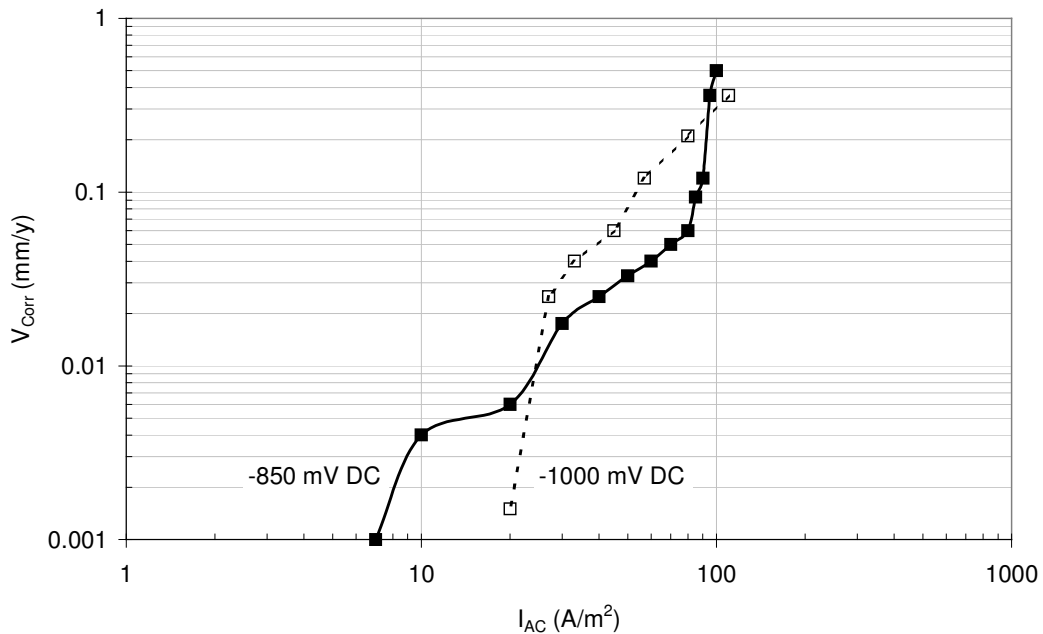


Figure 8. Corrosion rate versus AC current density – potentiostatic experiments.

As observed, the corrosion rate apparently increase with increasing current density in both experiments, but there seems to be some uncertainty of the effect of the increased

CP imposed in the 15h experiment. On one hand, the corrosion rate is observed to be greater in some current region in the -1000 mV DC case, but on the other hand, the corrosion decays faster when the AC current is lowered.

Another quite interesting observation is that the variation in the OFF-potential is greater in the -1000 mV experiment as shown in figure 9. It is evident that the OFF-potential in both experiments shows a quite constant variation. In the 70h experiment (-850 mV DC), the variation is in between -800 and -900 mV, whereas the variation in the 15h experiments is in between -700 and -1200 mV SCE. It is noted that although the anodic peaks of the OFF potentials are constant (-800 and -700 mV, the corrosion rate decreases to practically zero in both cases. From this is concluded that although it seems logical that the anodic peak potential may be another useful parameter (no corrosion as long as the peak potential does not become more anodic than a certain critical value) the anodic peak potential does not exclusively conduct the corrosion rate.

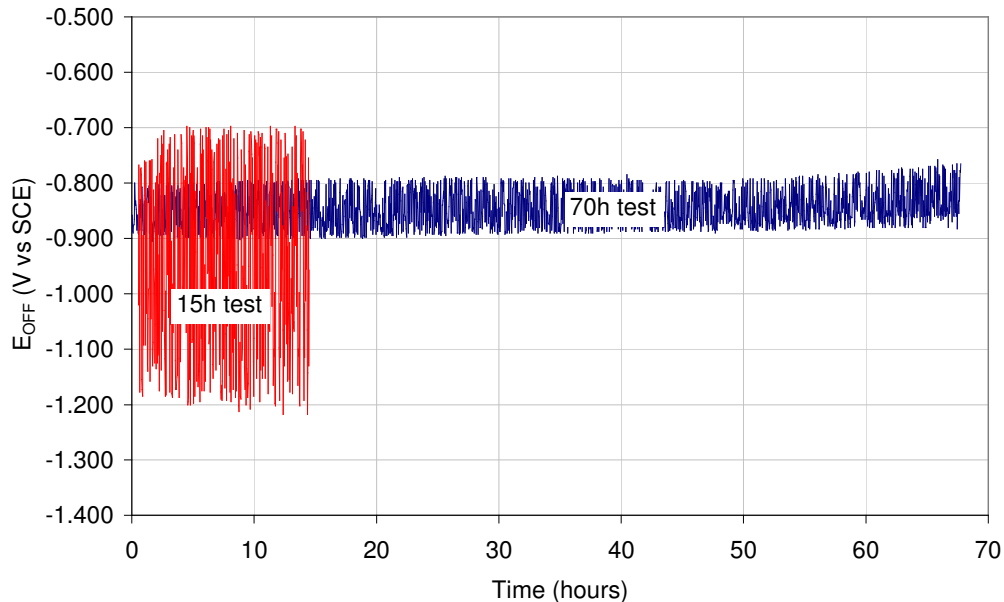


Figure 9. Variation of the OFF potentials throughout time in the potentiostatic experiments.

Galvanostatic experiments

In order to further the effect of the AC current density in particular on the corrosion rate, the galvanostatic experiments were initiated.

Figure 10 shows an example of the Ramlog current recordings and calculated RMS of the current density in the 100 A/m^2 experiment, documenting a quite accurate current measurement by the Ramlog. Figure 11 shows the corresponding Ramlog potential measurements. The ON-potential was measured just after initiation of the test and just prior to termination of the test using a fluke multimeter (initially -936 mV SCE, finally -800 mV SCE) showing a quite good agreement between the Ramlog average E_{ON} – measurement and the potential measured by a multimeter.

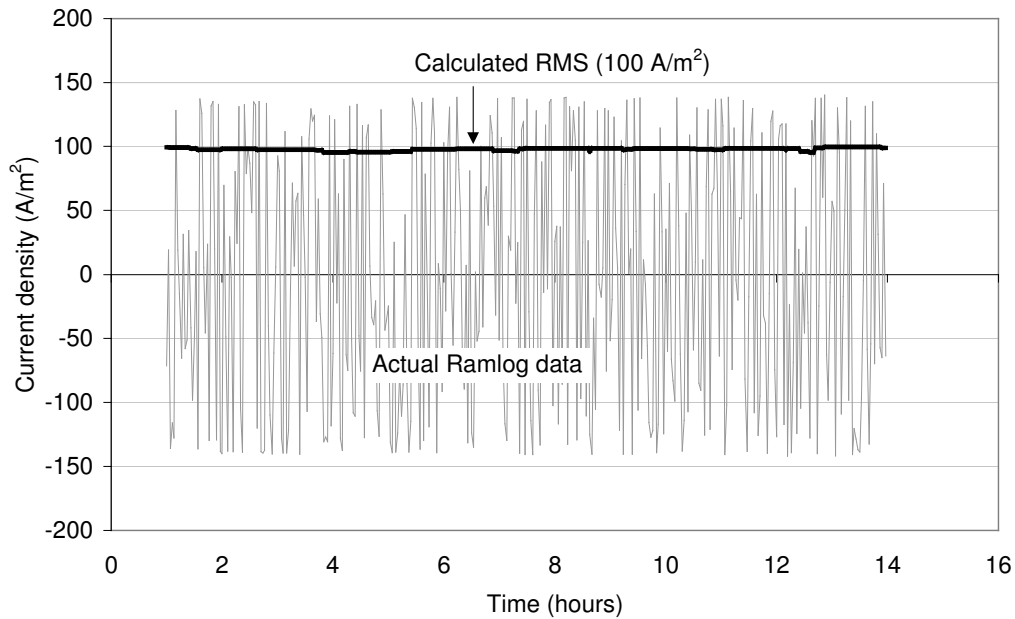


Figure 10. Ramlog recordings and calculated RMS of the current density in the 100 A/m^2 experiment.

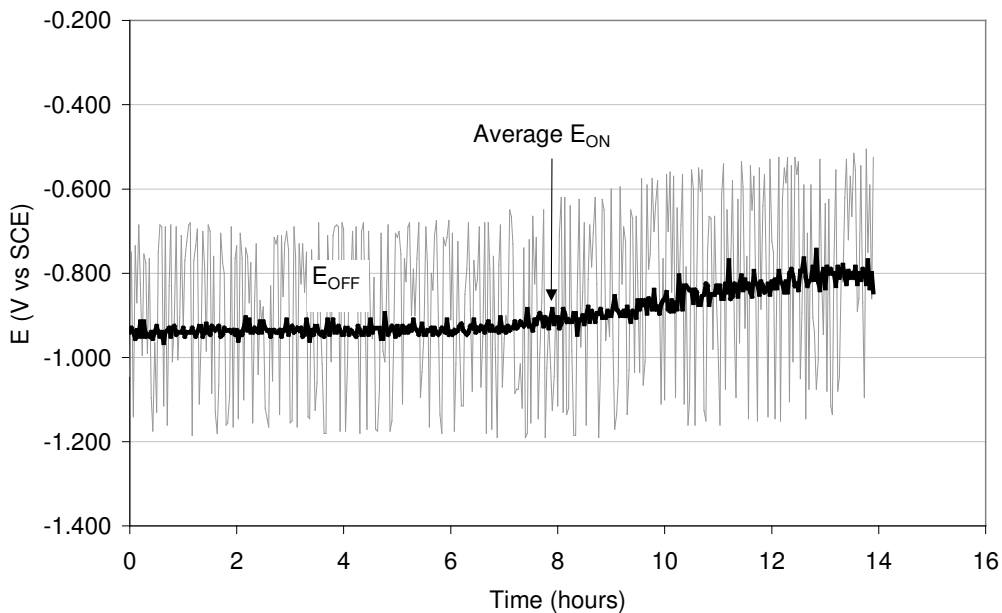


Figure 11. Ramlog recordings of the potential variation in the 100 A/m^2 experiment.

Figure 12 shows the correspondent ER-measurement. A quite consistent and well-defined increase in the probe resistance is observed from which the corrosion rate can be calculated on a minute by minute basis. Alternatively, the dashed line can be used to fit an average corrosion rate after some 2 hours of stabilisation. This line has a

slope of $32.7 \mu\Omega/\text{hour}$, which corresponds an average (but quite steady) corrosion rate of 0.12 mm/y .

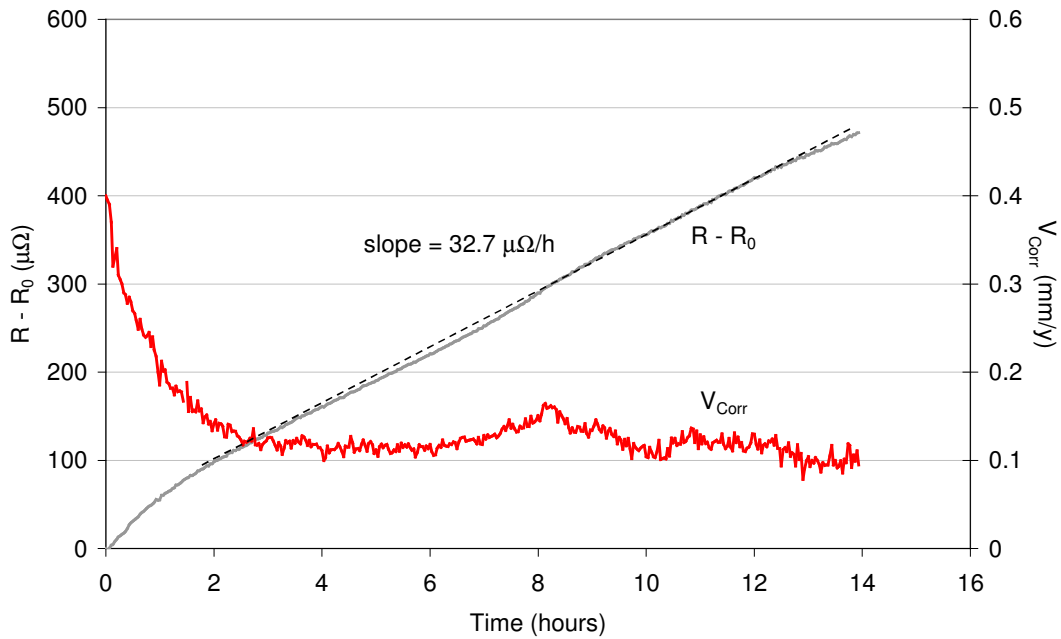


Figure 12. Result of the ER-corrosion rate measurement, 100 A/m^2 experiment.

By comparing the corrosion rates obtained for the five experiments with the applied constant AC current density, the data in table 2 are obtained.

No.	i_{DC} A/m^2	i_{AC} (RMS) A/m^2	V_{Corr} initial mm/y	V_{Corr} final mm/y
1	1	10	0.005	0.001
2	1	30	0.100	0.010
3	1	100	0.400	0.120
4	1	300	2.100	0.190
5	1	1000	6.250	2.450 (2h)

Table 2. Corrosion rates (initial and final) as a function of the applied AC current density.

The data of table 2 are presented graphically in figure 13. Note that both in table 2 and in figure 13, the final data for the heaviest AC current density (1000 A/m^2) is given after just 2 hours of exposure, since the ER-probe was destroyed by corrosion at this time.

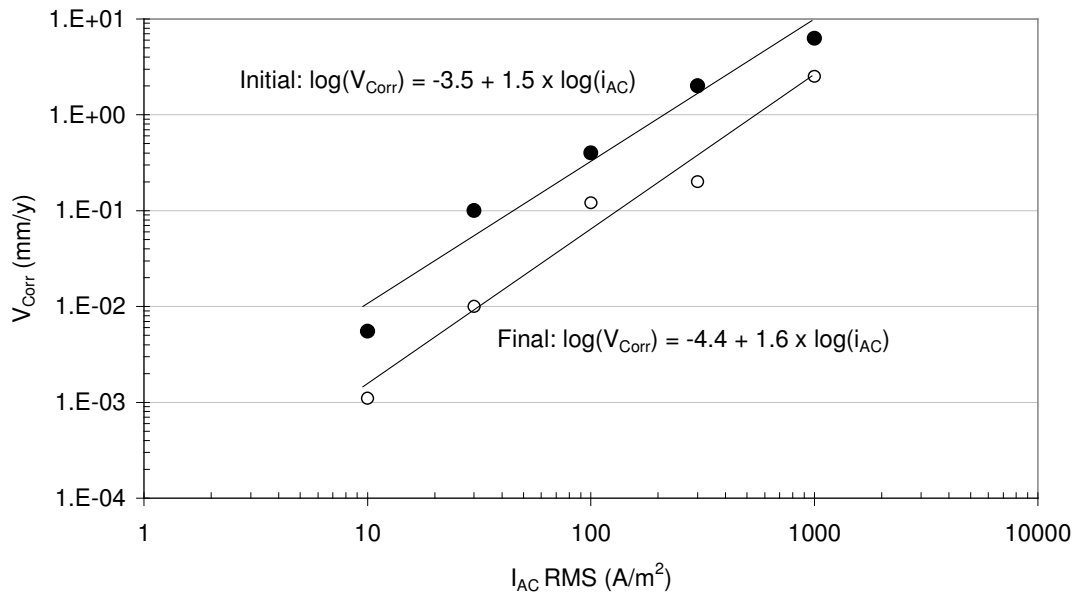


Figure 13. Corrosion rates versus AC current density in the galvanostatic experiments.

The initial and final corrosion rate values differ by around a decade, i.e. the corrosion rate decays over time. Initial values can be approximated by the trendline:

$$\log(V_{Corr}) = -3.5 + 1.5 \cdot \log(i_{AC}) \quad (4)$$

Final values are approximated by:

$$\log(V_{Corr}) = -4.4 + 1.6 \cdot \log(i_{AC}) \quad (5)$$

The decay in corrosion rate by a decade from initial to steady state corrosion is not at all unusual in traditional, general DC corrosion, and it seems quite natural that the same decay is observed when superimposed AC controls the corrosion conditions.

Figure 14 illustrates a comparison between the corrosion rates obtained in the galvanostatic- and in the potentiostatic experiments. It seems that the corrosion rates obtained in the potentiostatic experiments are located within the range established by the galvanostatic experiments, despite the difference in experimental conditions.

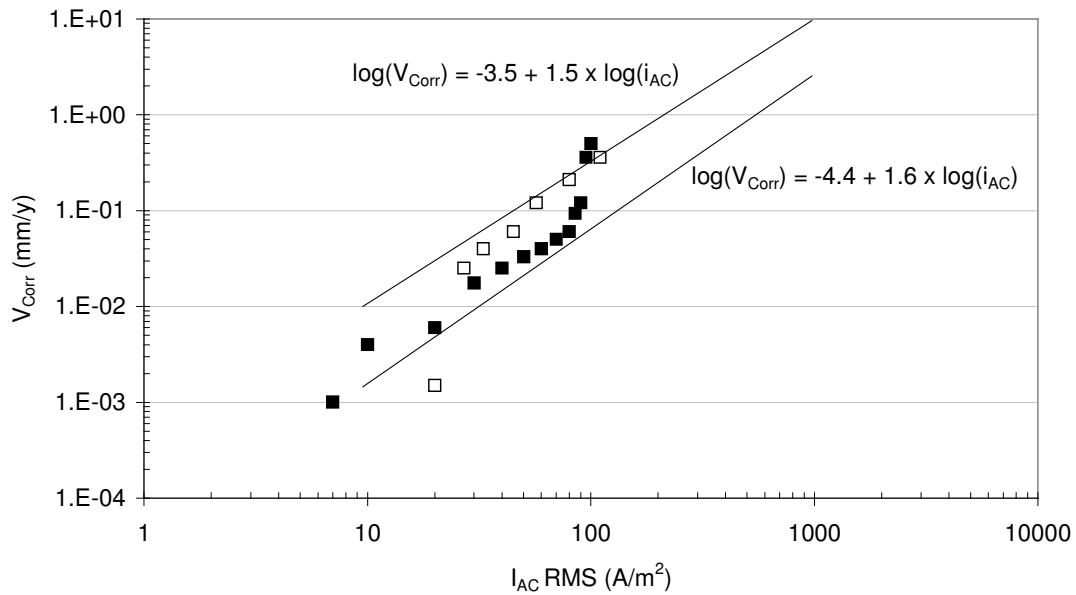


Figure 14. Comparison of corrosion rates obtained in the galvanostatic and in the potentiostatic experiments. Squares represent potentiostatic data from figure 8.

Regarding the effect on corrosion rate of the potential variation and in particular the anodic peak OFF-potential, it has been indicated from figure 9 (potentiostatic experiments) that although the variation in the OFF-potential was observed to be almost constant, the corrosion rate was ever decreasing in these experiments. The same trend is suggested from figure 11, showing that the anodic peak potential increases (shifts towards more anodic values) throughout the progress of the test period. At the same time, the corrosion rate (after a period of stabilisation) stays rather constant around 0.1-0.12 mm/y (figure 12). This shows again that although the anodic peak potential logically has some influence in the corrosion rate, the chemical conditions at the vicinity of the electrode surface may change in such manner that the steel is protected from corrosion – just like a passive surface in traditional DC-corrosion.

It has been shown previously⁸ that the increasing AC depolarises the DC behaviour of a steel electrode. In the present galvanostatic investigation, The ON-potential was measured by a multimeter in the beginning and at the end of the test period. These data are plotted in figure 15, showing that also in this case, the electrode is depolarised.

The effect of the anodic peak potential and the depolarisation phenomenon is discussed in greater detail elsewhere.⁹

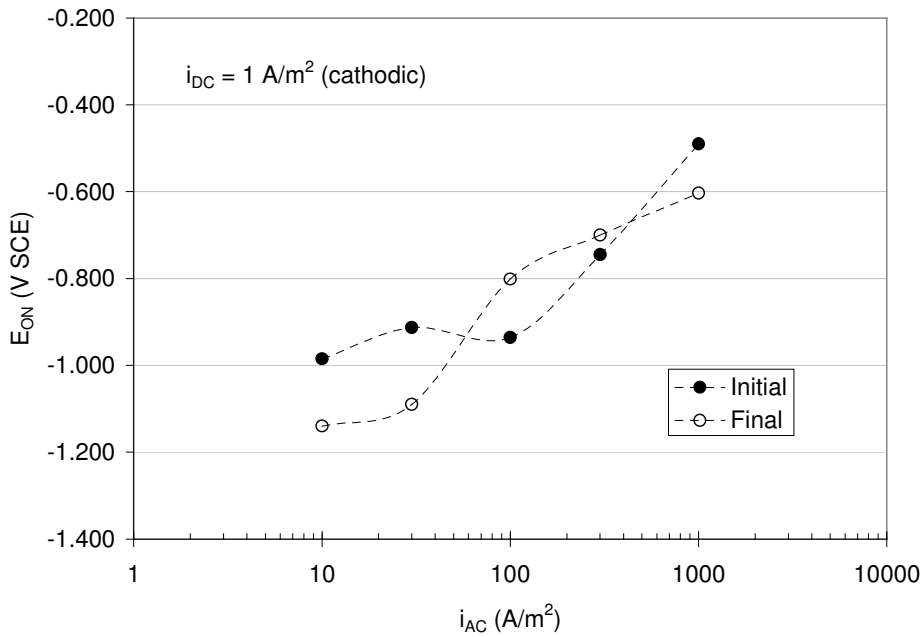


Figure 15. The effect of AC current on the ON-potential (initial and final values of E_{ON}).

Conclusions

- In an artificial solution with a capability of forming cathodic scaling throughout time, the corrosion rate of steel has been studied by the ER-technique under conditions with controlled AC and DC voltage as well as with controlled AC and DC current.
- The resulting AC current density in the controlled voltage experiments showed that the AC current density decreased throughout time due to development of increased spread resistance caused by the cathodic scaling. The scaling and accordingly the increase in spread resistance developed faster when increasing the degree of cathodic protection (DC potential -850 mV SCE versus -1000 mV SCE). The corrosion rate decreased throughout time as the AC current decreased due to the increased spread resistance.
- The controlled current experiments were initiated in order to study the corrosion rate when the AC current in particular was held constant (5 levels from 10-1000 A/m² was superimposed onto the constant DC of 1 A/m²). From these experiments, the thesis that the AC current density can be used to assess the degree of the AC corrosion risk was tested. The measured corrosion rates were found to fit into the general equation $\log(V_{Corr}) = -A + B \cdot \log(i_{AC})$.
- In the controlled current experiments, the initial corrosion rate was around one decade higher than the corrosion rate after 15h (representing values closer to a steady state condition), but both initial- and final corrosion rate was found to

increase with increasing AC current density following said equation. The corrosion rates measured in the controlled voltage experiments were found to be located in the range as defined by the controlled current experiments.

References

1. C.H.Voûte, F.Stalder, Influence of Alkaline and Earth Alkaline Cations on the Development of Spread Resistance on Cathodically Protected Coupons, Booklet on AC corrosion presented in Proceedings CeoCor2000.
2. C.H. Voûte, F. Stalder, Einfluss der Bodenzusammensetzung auf den Aufbreitungswiderstand und die Wechselstromkorrosion von katodisch geschützten Messproben, Proceedings CeoCor2000.
3. A. Pourbaix, P. Carpentiers, and R. Gregoor, Detection and Assessment of Alternating Current Corrosion, *Materials Performance*, 39 (3), pp. 34-37, 2000. Also presented in Proceedings Ceocor2000.
4. L.V. Nielsen, Thermodynamical Considerations on the Local Chemistry Formed at the Steel-Soil Interface of Cathodically Protected Pipelines, Paper 1, this report.
5. L.V. Nielsen, Comparison of EIS and Ramlog Measurements of Spread Resistance and Polarisation Impedance for Steel Exposed in Scaling and Non-Scaling Solutions at 50 Hz AC, Paper 4, this report.
6. L.V. Nielsen, K.V. Nielsen, Measurement of Accumulated Corrosion and Instant Corrosion Rate using a Refined Electrical Resistance Technique. Internal Report.
7. Method and Apparatus for Measuring Accumulated and Instant Rate of Material Loss or Material Gain, Danish Patent Application PA 1999 01772.
8. L.V. Nielsen, Effects of 50 Hz AC on the DC Polarisation Behaviour of Steel Exposed in Artificial Soil Solutions. Paper 5, this report
9. L.V. Nielsen, AC Corrosion Rates of Cathodically Polarised Steel Exposed in a Non-Scaling, Neutral pH Soil Solution, Paper 7, this report.